Nonadiabatic transition in $n = 2$ atomic hydrogen

R. D. Hight* and R. T. Robiscoe
Physics Department, Montana State University, Bozeman, Montana 59175
(Received 27 October 1977)

We present an experiment studying the nonadiabatic passage of the $F = 1$ hyperfine component of the $2\,^2S_{1/2}$ metastable state of atomic hydrogen through a reversing solenoidal magnetic field. The nonadiabatic region is compared to the model field of Hight, Robiscoe, and Thorson. The measured transition amplitudes are fitted by the calculated amplitudes and the results are discussed.

I. INTRODUCTION

In previous measurements of the fine-structure intervals in the $n = 2$ level of atomic hydrogen by an atomic-beam method, a state-selection technique was used.[1,2] Briefly, an atomic beam was produced containing metastable $2\,^2S_{1/2}$ atoms in the $F = 1, m = +1$ and 0 states only. This beam then passed through a solenoid, where the current was adjusted so that the ambient magnetic field was brought to zero. As the field went to zero, transitions were induced to the $2\,^2S_{1/2}(F = 1, m = -1)$ state, called the $\beta(B)$ state, which was used as a single initial state for subsequent radio-frequency transitions to the $2P$ states. Two peculiarities were noted about the production of the $\beta(B)$ state.[3,4] First, a measurement of the $\beta(B)$ state population as a function of solenoid current, i.e., transition magnetic field strength, produced a curve with oscillatory structure. Second, a measurement of the velocity distribution of the $\beta(B)$ state again showed oscillatory structure. The question of the nature of the transitions between the $F = 1$, $m = +1$, and $m = 0$ states and the $\beta(B)$ state was thus raised.

The present authors, with Thorson, have recently investigated the nonadiabatic passage of an oriented spin through a model inhomogeneous magnetic field in an attempt to explain the observed phenomena.[5] The model was fashioned after Majorana's model, which considered the passage of an oriented spin near the neighborhood of a zero field point.[6] This model interaction, similar to the Landau-Zener-Stueckelberg (LZS) model for curve crossings in collision theory, was chosen because of its resemblance to the magnetic field interaction in the previous experiments.[1,2] Solutions for the final-state populations were found for the nonadiabatic passage of a spin-one particle. Agreement between theory and the original experimental data was not good, however; this was attributed to the presence in the original experiments of a second "accidental" nonadiabatic transition region not easily modeled. In this paper, we present the results of a new experiment where the transition region was designed to more closely approximate the LZS model in order to better test the theory.

In this experiment, a beam containing metastable $2\,^2S_{1/2}$ atoms with a population equally distributed between the $F = 1, m = +1$ and $F = 1, m = 0$ hyperfine-structure states is produced by standard techniques.[1,2] The beam passes adiabatically from the production region to the transition region. The transition region, which we call a "flopper," consists of two oppositely wound current-carrying solenoids butted together. The beam travels down the axis of the flopper where the predominantly axial magnetic field passes through zero and reverses direction. The magnetic field coupling between the metastable hyperfine-structure states is in a reasonable approximation to the LZS-model coupling. The beam then travels adiabatically through a state selector and the fractional population of the $\beta(B)$ state $(F = 1, m = -1)$ induced by passage through the flopper is selectively detected. The $\beta(B)$ time-of-flight distribution is also measured in order to measure the $\beta(B)$ velocity distribution.

The experimental techniques for production and detection of such a metastable beam are well known and extensively discussed in the literature.[1-4,7] Only the transition region or "flopper" will be discussed in detail in Sec. II. In Sec. III, the experimental data and the theoretical state populations will be given and discussed before being compared; later, a comparison incorporating experimental averaging effects due to finite size and beam velocity distribution will be discussed. We give our summary and conclusion in Sec. IV.

II. TRANSITION REGION

The transition region or "flopper" consists of two oppositely wound solenoids on a brass spool with a 1.06-cm-diam hole bored down the axis. Each solenoid is wound with 640 turns of 27-gauge magnetic wire and has a mean radius of 0.99 cm and a length of 7.5 cm. The spool is mounted inside a cylindrical soft iron shield with 1.27-cm-

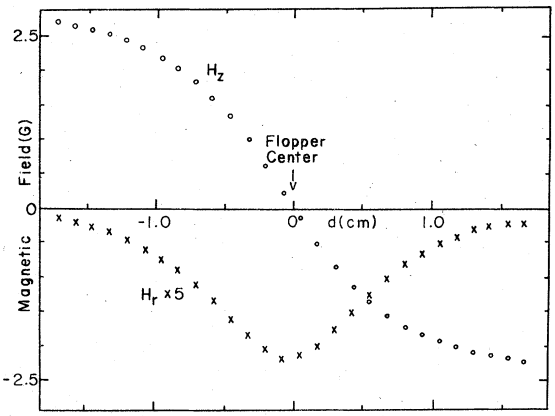

FIG. 1. The axial (H_z) and transverse (H_r) magnetic fields as functions of distance, 2 cm either side of the center of the floppers with 25 mA of current.

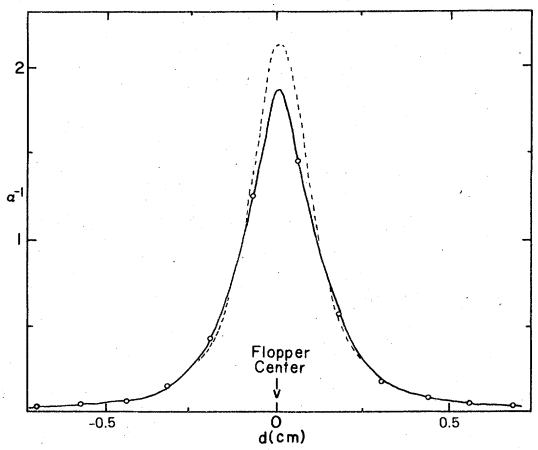

FIG. 2. The inverse adiabaticity parameter for the magnetic field in Fig. 1.

diam beam entry and exit holes coaxial with the flopper. Additional shielding is provided by three layers of Conetic and two layers of Netic shielding material inside the iron cylinder. The shielding is required to eliminate the large static magnetic fields used in both the beam production and state analysis regions. The measured solenoid constant is 0.107 G/mA of current.

In Fig. 1, we show the axial and transverse magnetic fields as a function of axial distance near the center of the flopper, where the axial field direction rotates by π rad. These fields were measured along a line 0.28 cm off the flopper axis and for 25 mA solenoid current. Comparison of these fields with the LZS model fields used by Hight, Robiscoe, and Thorson (HRT) shows relatively poor agreement.[5] However, as discussed by HRT, the effective coupling between atomic states produced by passage through such inhomogeneous magnetic fields may be characterized overall by an "adiabaticity parameter" α, which is defined as the ratio of the spin Larmor frequency ω_L to the field rotation $d\theta/dt$ in the rest frame of the atom, where θ is defined as the angle which the field makes with respect to initial spin quantization axis. As we shall see, the experimental adiabaticity parameter for the fields of Fig. 1 shows relatively good agreement with the LZS model parameter used by HRT.

The field rotation rate $d\theta/dt$ may be transformed to a spatial rotation rate $d\theta/dz$ by introducing the atomic beam velocity v. For the case of our flopper, with two long, oppositely wound solenoids, the adiabaticity parameter may be approximated near the flopper center by

$$\alpha = \alpha_0 \rho^2 / \sin^3\theta .$$

This expression was used by HRT in their LZS-model calculation.[5] Here the parameter $\alpha_0 = \omega_L R/v$, where ω_L is the spin Larmor frequency, v is the atom velocity, and R is the mean solenoid radius, which is related to the slope of the axial field as it reverses direction. The parameter ρ is defined as the atom's distance off the flopper axis divided by $2R$. The flopper transverse magnetic field near the axis is determined mainly by the ρ value while the axial field is assumed independent of ρ.

The adiabaticity parameter α is smaller by several orders of magnitude in the nonadiabatic region (near the flopper center) as compared with the adiabatic region (away from flopper center). Thus, for convenience, we show in Fig. 2 a plot of the *inverse* of α as a function of axial distance on either side of the zero axial-field point, for an assumed beam velocity of 1×10^6 cm/sec. The experimental points are fitted quite well by the theoretical expression for $1/\alpha$ (the solid line) if an effective ρ value is choosen to be 1.07 times the measured ρ value. As mentioned above, the experimental and theoretical values for α agree much better than do the experimental and LZS-model magnetic fields. Since we expect transitions to be induced mainly in the region of large values of $1/\alpha$ and the transition probability to be predominantly controlled by the value of α, we conclude that our flopper provides a reasonable experimental approximation to the LZS model used in the HRT calculation.[5]

During the experiment, we measured the axial transverse magnetic fields along the entire beam axis from production to detection regions. In this way, we discovered a second well-localized nonadiabatic region near the entrance to the flopper, in addition to the primary nonadiabatic region at the center of the flopper. This spurious nonadia-

batic region arises from the production region where a transverse field of the order of 600 G must be rotated to an axial field of a few gauss upon entrance to the flopper. Due to design limitations, it was not possible to accomplish this rotation adiabatically. Thus, instead of trying to eliminate the spurious region, we made it as nonadiabatic as possible ($\alpha < 0.15$) over the range of field strengths used in the flopper. The major effect of the spurious region was then to change the initial $2\,^2S_{1/2}$ state populations upon passage through the primary nonadiabatic region from the $m=+1$ and $m=0$ states equally populated to the $m=-1$ and $m=0$ states equally populated. This sudden spin inversion is important later when we discuss the phase relations between the various m states generated by their coupling to the magnetic field. Finally, our field measurements also showed that with zero current through the flopper solenoids and all other fields at typical operating points, there was present in the flopper a residual axial field of 0.25 G. This is also significant in the data analysis of Sec. III.

III. DATA AND ANALYSIS

Figure 3 shows a typical $\beta(B)$ "production curve," i.e., the fractional $\beta(B)$ population relative to the total $2\,^2S_{1/2}$ population as a function of current in the flopper. Figure 4 shows a typical time-of-flight curve for the $\beta(B)$ state taken immediately after the production curve. In principle, the structure on both curves may be enhanced in two ways: by reducing the transverse dimensions of the beam (appropriate beam collimation), and by reducing the beam's natural thermal-velocity distribution (suitably gating the detector). We tried both methods, but the structure of the curves was not appreciably improved because of low signal-to-noise

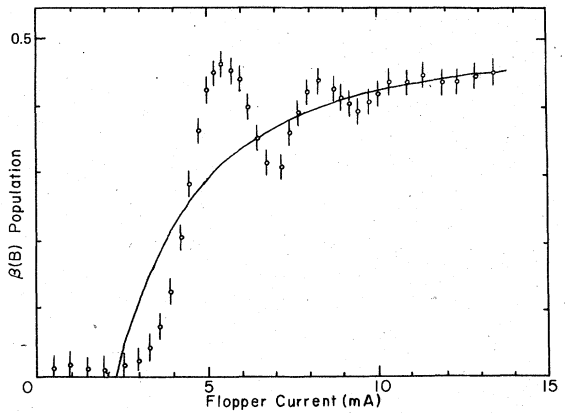

FIG. 3. The $\beta(B)$ state population indicated by the circles as a function of the flopper current with the dark line the LZ term fit.

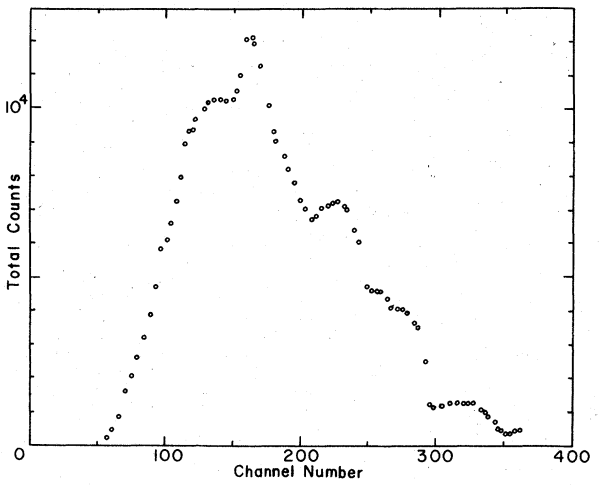

FIG. 4. The time-of-flight distribution of the $\beta(B)$ state with a flopper current of 27.5 mA and 0.59 μsec/channel.

ratios. Thus we must average the theoretical $\beta(B)$ population over both the beam velocity distribution and the finite beam size. We discuss these averaging procedures later in this section.

Immediately, we note that no transitions are induced until the flopper current reaches about 2 mA. The residual magnetic field requires 2.3 mA of current before the axial field is driven to zero and reverses direction. We also note that the previously mentioned spurious region did not appear either until this current was reached. From this current on, the spurious crossing point remained nonadiabatic until a current of 50 mA was reached and α became greater than 0.15. The net effect of the residual field is to cause an offset in the current of 2.3 mA.

The induced $\beta(B)$ state population from HRT with the initial conditions that the $F=1$, $m=-1,0$ states are equally populated is

$$\beta(B) = \tfrac{1}{2}(1-e^{-A}) - \sqrt{2}\,e^{-A/4} \times (1-e^{-A/2})^{3/2}\cos(\lambda_\pi - \phi), \tag{1}$$

where $A = \pi\alpha_0\rho^2$ and

$$\lambda_\pi = \int_0^{\pi/2} \alpha(\theta)\,d\theta.$$

The value of α varies smoothly from $\pi/4$ to zero as A increases from zero to infinity. The argument λ_π as defined above diverges and is not applicable as discussed by HRT. We shall use a finite cutoff method similar to that discussed by HRT but with one modification. The model defines a cutoff point $Z_0 = R$, the mean solenoid radius; however, since our fields do not exactly coincide with the model, we assume the cutoff point to be a variable of the order of R. The in-

tegration for λ_π then yields $\lambda_\pi = \alpha_0 \zeta(Z_0, \rho)$, where

$$\zeta(Z_0, \rho) = [Z_0(Z_0^2 + \rho^2 R^2)^{1/2} + (\rho R)^2 \times \ln\{[Z_0 + (Z_0^2 + \rho^2 R^2)^{1/2}]/\rho R\}]/2R^2. \quad (2)$$

The $\beta(B)$ state population (Eq. 1) is the sum of two terms that may be treated separately. The first term on the right hand side of Eq. 1 is a smooth nonoscillatory function independent of Z_0. We choose to denote this term as A_{LZ} because of its similarity to the Landau-Zener (LZ) level crossing solution. The second term is a damped oscillatory function that is dependent upon Z_0. This term is referred to simply as the oscillatory term (osc). This simplifies the analysis of the data as each can be averaged separately and the LZ term subtracted to yield the oscillatory portion. The averaging over the beam size assumes a uniformly dense circular cross section with a maximum radius defined by $\rho_0 = r_0/2R$. The term A_{LZ} may be integrated to yield

$$\bar{A}_{LZ} = [1 - (1 - e^{-A_0})/A_0], \quad (3)$$

where $A_0 = \pi \alpha_0 \rho_0^2$. The osc term could not be integrated analytically and therefore was performed numerically. The velocity averaging was also done numerically by fitting the time-of-flight distribution of the $2\,^2S_{1/2}$ state with a Gaussian function and then integrating. We found that the velocity averaging of A_{LZ} yielded results within 0.5% of those obtained by simply evaluating α_0 at the peak time of flight τ_0 ($v_0 = d/\tau_0$, where d is the distance from production to detection). Therefore we used Eq. 3 with α_0 evaluated at τ_0 to curve fit the $\beta(B)$ production curve as shown by the solid line in Fig. 3. We allowed ρ_0 to vary to obtain the best fit and then used ρ_0 in the averaging of the oscillatory term. The term A_{LZ} was then subtracted from the data and is shown in Fig. 5. The solid line is the theoretical fit found by varying Z_0. The value of ρ_0 was taken from the LZ term fit and τ_0 was found experimentally from the time-of-flight (TOF) distribution. Table I summarizes the results from three typical runs with different peak times-of-flight.

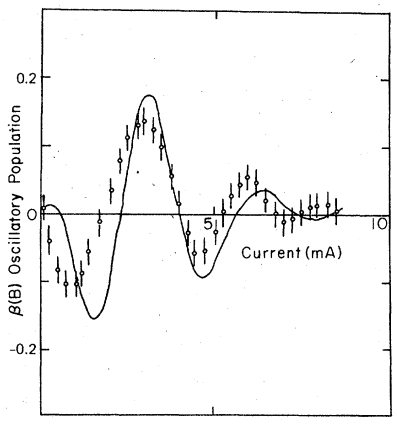

FIG. 5. The oscillatory portion of the $\beta(B)$ state population of Fig. 3 with the dark line the best fit with $\tau_0 = 95$ μsec, $\rho_0 = 0.50$, and $z_0 = 1.80$ cm.

TABLE I. Data summary table.

Flopper curves	ρ_0	Z_0(cm)	τ_0(μsec)
I	0.50 ± 0.01	1.80 ± 0.05	95.0
II	0.53 ± 0.01	1.81 ± 0.05	97.0
III	0.51 ± 0.01	1.77 ± 0.05	100.0
Averaged	0.51 ± 0.02	1.79 ± 0.05	

The averaged experimental values of 0.51 for ρ_0 and 1.79 cm for Z_0 are approximately twice the expected values of 0.27 and 0.99 cm, respectively. As a check on these values for ρ_0 and Z_0, the period for the oscillations observed in the TOF distributions were calculated using these values. The calculated periods were within 8% of the observed periods: this indicates good agreement considering the small amplitudes of the TOF oscillations. The period of the TOF oscillations could not be determined to better than 10%.

The fact that ρ_0 and Z_0 are approximately twice as large as expected is surprising. We attempted to explain the discrepancy of ρ_0 by varying the beam cross-section density and shape. We could not bring the values of ρ_0 closer to the expected 0.27. Assuming misalignment between the beam and flopper also gave no improvement. Even rounding off the "corners" of the model field (so there is a smooth transition from adiabatic to nonadiabatic and back again) gave no significant change in ρ_0. At present this discrepancy is unresolved and we are inclined to blame the spurious nonadiabatic region. The fact that Z_0 is also about twice as large as expected may not be surprising since our analysis to this point does not take into account the smooth transition between adiabatic and nonadiabatic regions. The interesting point here is that HRT predict that the period of the oscillations should be dominated by the adiabatic region prior to entry. The reason is that the accumulated relative phase between the substates is linear in the applied field and hence the current. An order of magnitude calculation yields oscillations due to this accumulated phase of about $\frac{1}{8}$ the observed period or the period due to the nonadiabatic region. It is not clear why we do not observe these high-frequency oscillations. We can say, however, that the presence of the spurious nonadiabatic region complicates the determination of

the initial phases of the $m_F = 0$ and -1 amplitudes, and it may destroy the oscillations in question.

IV. CONCLUDING REMARKS

We conclude that we have achieved semiquantitative understanding in detail of nonadiabatic transitions in inhomogeneous magnetic fields. The experimental data can be fitted by the model of HRT. The discrepancies between the experimental values for ρ_0 and Z_0 and the theoretical values may be due to the spurious nonadiabatic region. Efforts to eliminate this region are continuing in the hope of obtaining better agreement with theory. Presently, the other state populations ($F = 1, m_F = +1, 0$) are being investigated to see if they too argue with the model of HRT.

ACKNOWLEDGMENTS

The authors wish to thank the National Bureau of Standards for financial support from the Precision Measurements Grant No. 4-9004.

---

*Present address: Department of Physics and Astronomy, University of Nebraska, Lincoln, Neb. 68588.

[1]R. T. Robiscoe, Phys. Rev. 138, A22 (1965).
[2]T. W. Shyn, T. Rebane, R. T. Robiscoe, and W. L. Williams, Phys. Rev. A 3, 116 (1971).
[3]T. Rebane, Ph.D. thesis (University of Michigan, 1970) (unpublished).
[4]R. D. Hight, Ph.D. thesis (Montana State University, 1974) (unpublished).
[5]R. D. Hight, R. T. Robiscoe, and W. R. Thorson, Phys. Rev. A 15, 1079 (1977).
[6]E. Majorana, Nuovo Cimento 9, 43 (1932).
[7]R. T. Robiscoe, in *Cargese Lectures in Physics* (Gordon and Breach, New York, 1968), pp. 3–53.